Available online at www.sciencedirect.com
SCIENCE DIRECT®
Journal of Sound and Vibration 285 (2005) 637–652
JOURNAL OF SOUND AND VIBRATION
www.elsevier.com/locate/jsvi

Dynamic stability of a sandwich plate with a constraining layer and electrorheological fluid core

Jia-Yi Yeh, Lien-Wen Chen*

Department of Mechanical Engineering, National Cheng Kung University, Tainan 70101, Taiwan, Republic of China

Received 30 October 2003; received in revised form 25 June 2004; accepted 26 August 2004
Available online 2 December 2004

Abstract

The dynamic stability problems of a sandwich plate with a constraining layer and an electrorheological (ER) fluid core subjected to an axial dynamic force are investigated. The rectangular plate is covered in an ER fluid core and a constraining layer to improve the stability of the system. Effects of the natural frequencies, static buckling loads, and loss factors on the dynamic stability behavior of the sandwich plate are studied in the paper. Rheological property of an ER material, such as viscosity, plasticity, and elasticity may be changed when applying an electric field. The modal damper and the natural frequencies for the sandwich plate are calculated for various electric fields. When an electric field is applied, the damping of the system is more effective. In this study, finite element method and the harmonic balance method are used to calculate the instability regions of the sandwich plate. The ER fluid core is found to have a significant effect on the dynamic stability regions.

1. Introduction

When a structure is subjected to periodic loads, it is well known that the ordinary forced response will lead to dynamic instability under some circumstances. The induced violent vibration is called the dynamic instability or parametric resonance. A number of investigators have studied the dynamic instability due to periodic loads: two of these are Bolotin [1] and Evan-Iwanowski [2].

*Corresponding author. Tel.: +886 6 275 7575; fax: +886 6 235 2973.
E-mail address: chenlw@mail.ncku.edu.tw (L.-W. Chen).

0022-460X/$ - see front matter © 2004 Elsevier Ltd. All rights reserved.
doi:10.1016/j.jsv.2004.08.033

The periodic loads may cause parametric vibrations, which may damage the structures. As a consequence, the dynamic instability of a structure subjected to periodic compressive loads has attracted a lot of attention. The dynamic stability analyses of the rectangular plate have been widely investigated. Bolotin [1] presented comprehensive studies for the dynamic stability of the machine components and the structural members. Briseghella and Pellegrino [3] investigated the dynamic instability problems of elastic structures by finite element method. Takahasi and Konishi [4] studied the dynamic instability of the rectangular plates subjected to a linearly distributed load, such as pure bending, along the two opposite edges using harmonic balance method. The parametric instability characteristics of rectangular plates subjected to localized edge compressing (compression or tension) are solved by Deolasi and Datta [5]. They studied the dynamic stability of thin, square, isotropic plates with simply supported boundary conditions, using finite element method.

Srinivasan and Chellapandi [6] investigated the dynamic instability of a rectangular laminated composite plate. Moorthy and Reddy [7] solved the parametric instability problems of the laminated composite plates with transverse shear deformation. Then, Chen and Yang [8] studied the dynamic stability problems of the laminated plates by the finite element method.

Many studies regarding the active control of structural vibration have so far been devoted to the use of electrorheological (ER) fluids. ER fluids have great potential in applications for intelligent materials and structures. The ER fluid has the same properties as a viscoelastic material at small strain level. A detail review of ER material advancement was presented by Weiss et al. [9]. The damping of the ER fluids has been paid attention by many researchers since Brooks et al. [10] studied the viscoelastic property of the ER fluids. Choi and Park [11] and Choi et al. [12] studied the vibration characteristics of a composite beam with an ER fluid. Oyadiji [13] showed that the modal parameters were more dependent on the location and size of the ER fluid constraining layer damping treatment than on the electric field strength for an aluminum plate. The use of an ER fluid for the construction of smart components has been previously suggested and investigated in the Coulter's investigation [14]. The more detail investigations of the ER material in the structural vibration can be traced to Yalcintas and Coulter [15,16] and Yalcintas and Dai [17]. They studied the vibration problem of a sandwich beam with an ER fluid core and discussed the effects of the thickness and loss factor on the vibrations were also presented. Then, Lee [18] investigated the transverse free vibration problem of a sandwich beam, where an iterative method was explored to study the properties of the nonlinear ER fluid. Kang et al. [19] studied the passive and active damping characteristics of smart ER composite beams. They investigated the flexural vibration of laminated composite beams sandwiched by two ER fluid layers to maximize the possible damping capacity.

In the present study, the dynamic stability of a sandwich plate with a constraining layer and ER fluid core is investigated. To the author's knowledge, no work has done to study the vibration and the dynamic stability of a sandwich plate with a constraining layer and ER fluid core. The finite element method and the harmonic balance method are adopted to obtain the instability regions of the sandwich plate and the effects on the instability regions of the constraining layer and ER layer are also discussed in the paper. By using the complex modulus representation of the ER material, the Mathieu equation with complex coefficients is obtained. Then the significant effects on the behavior of the sandwich plate are found in this study.

2. Problem formulation

The structure of a sandwich plate with a constraining layer and an ER fluid core is demonstrated in Fig. 1. Layer 3 is a pure elastic, isotropic and homogeneous constraining layer. Layer 2 is an ER fluid material and the properties of the ER material can be changed by applying different electric fields. The base plate is assumed to be undamped, isotropic and homogeneous and is designated as the layer 1. Before the derivation procedures, the other assumptions used in this study must be mentioned:

1. No slipping between the elastic and ER layers is assumed.
2. The transverse displacements, w, of all points on any cross-section of the sandwich plate are considered to be equal.
3. There exists no normal stress in the ER layer, and there exists no shear strain in the elastic layer either.

By referring to Fig. 2, the strain–displacement relation of the elastic layer can be expressed as:

$$\varepsilon_{xi} = \frac{\partial u_i}{\partial x} - z_i \frac{\partial^2 w}{\partial x^2},$$

$$\varepsilon_{yi} = \frac{\partial v_i}{\partial y} - z_i \frac{\partial^2 w}{\partial y^2}, \quad i = 1, 3, \tag{1}$$

where ε_{xi} and ε_{yi} are the bending strains, u_i and v_i are the axial displacements of the mid-plane of layer i at the x and y directions, respectively, and z_i is the distance of the mid-height of layer i.

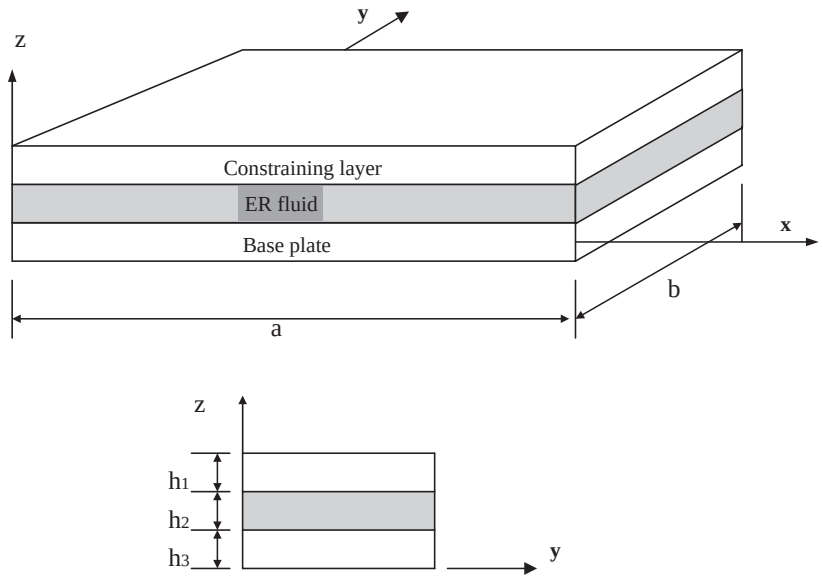

Fig. 1. The sandwich plate with an ER fluid core and a constraining layer.

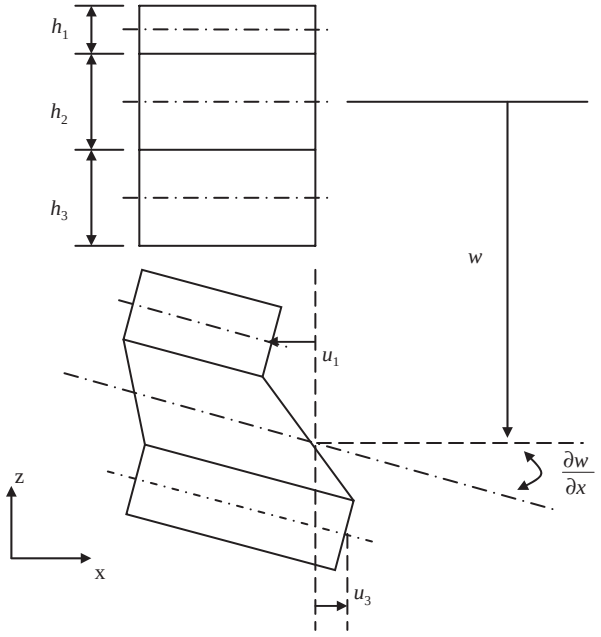

Fig. 2. Undeformed and deformed configurations of a sandwich plate.

Considering the strain–displacement relation of the ER layer, the shear deformation can be further expressed as

$$\gamma_{x2} = \frac{\partial w}{\partial x} + \frac{\partial u_2}{\partial z}, \tag{2}$$

$$\gamma_{y2} = \frac{\partial w}{\partial y} + \frac{\partial v_2}{\partial z}, \tag{3}$$

where u_2 and v_2 are the axial displacements in the x and y directions of the ER layer, respectively. By referring to the geometric relationship between u_1, u_3, v_1, v_3 and $\partial w/\partial z$ of the face-plate (as shown in Fig. 2), it can be obtained that

$$\frac{\partial u_2}{\partial z} = \frac{h_1 + h_3}{2h_2}\frac{\partial w}{\partial x} + \frac{u_1 - u_3}{h_2}, \tag{4}$$

$$\frac{\partial v_2}{\partial z} = \frac{h_1 + h_3}{2h_2}\frac{\partial w}{\partial y} + \frac{v_1 - v_3}{h_2}, \tag{5}$$

where h_1, h_2, and h_3 are the thickness of layers 1, 2, and 3, respectively.

Imposing the displacement compatibility (as shown in Fig. 3) through the thickness, the following shear strain in the mid-plane can be rewritten as

$$\gamma_{x2} = \frac{d}{h_2}\frac{\partial w}{\partial x} + \frac{u_1 - u_3}{h_2}, \tag{6}$$

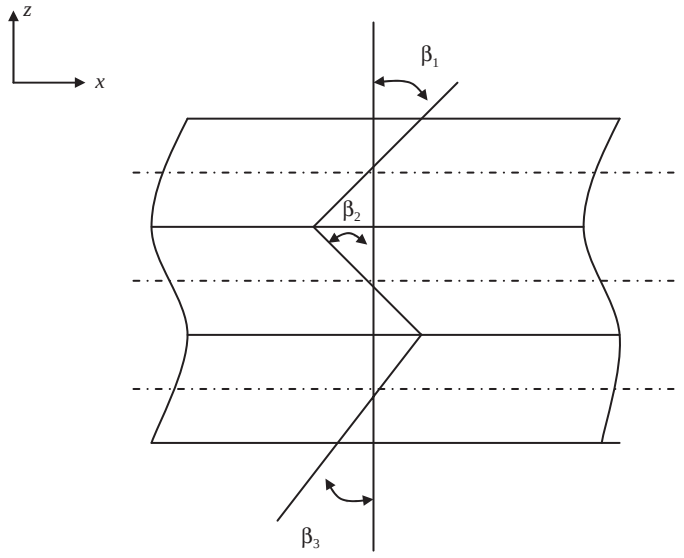

Fig. 3. Compatibility relation of systems.

$$\gamma_{y2} = \frac{d}{h_2}\frac{\partial w}{\partial y} + \frac{v_1 - v_3}{h_2}, \tag{7}$$

where

$$d = \frac{h_1}{2} + h_2 + \frac{h_3}{2}.$$

The strain energy associated with the normal strain in the elastic layer can be obtained:

$$V_i = \frac{1}{2}\int_V D_i(\varepsilon_{xi}^2 + \varepsilon_{yi}^2)\,\mathrm{d}v, \quad i = 1, 3, \tag{8}$$

where D_i is the differential operator matrix and listed in the following discussion in detail.

Then the strain energy of the ER layer is obtained as follows:

$$V_2 = \int_V G_2(\gamma_{x2}^2 + \gamma_{y2}^2)\,\mathrm{d}v, \tag{9}$$

where G_2 denotes the shear modulus of the ER fluid layer.

Let V be the total strain energy of the sandwich plate; then

$$V = V_1 + V_2 + V_3. \tag{10}$$

The kinetic energy of the sandwich plate has the following three parts:

1. The kinetic energy associated with the axial displacement:

$$T_1 = \frac{1}{2}\int\int_A [\rho_1 h_1(\dot{u}_1^2 + \dot{v}_1^2) + \rho_3 h_3(\dot{u}_3^2 + \dot{v}_3^2)]\,\mathrm{d}x\,\mathrm{d}y. \tag{11}$$

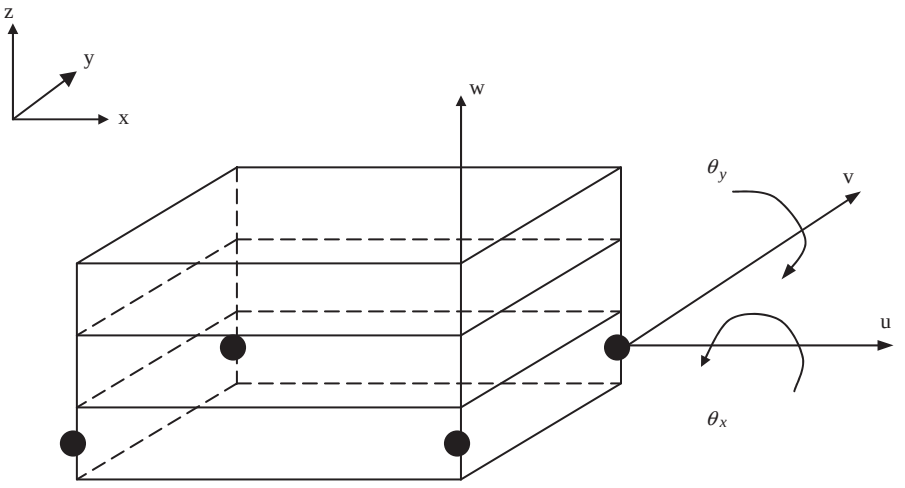

Fig. 4. A sandwich plate element with four end nodes and five dof per node.

2. The kinetic energy associated with transverse displacement:

$$T_2 = \frac{1}{2}\int\int_A (\rho_1 h_1 + \rho_2 h_2 + \rho_3 h_3)\dot{w}^2 \,\mathrm{d}x\,\mathrm{d}y. \tag{12}$$

3. The kinetic energy associated with the rotation of the ER layer:

$$T_3 = \frac{1}{2}\int\int_A I_2(\dot{\gamma}_{x2}^2 + \dot{\gamma}_{y2}^2)\,\mathrm{d}x\,\mathrm{d}y, \tag{13}$$

where I_2 is the mass moment of inertia of the ER layer.

Let T be the total kinetic energy of the sandwich plate, then

$$T = T_1 + T_2 + T_3. \tag{14}$$

The plate elements used in this study are two-dimensional element bounded by four nodal points. The plate element is shown in Fig. 4. Each node has seven degrees of freedom to describe the longitudinal displacements, transverse displacements, and slopes of the sandwich plate. The transverse displacement, longitudinal displacement can be expressed in terms of a nodal displacement vector and a shape function vector:

$$w(x,y,t) = N_w(x,y)\{q(t)\}, \tag{15}$$

$$u_1(x,y,t) = N_{u1}(x,y)\{q(t)\}, \tag{16}$$

$$u_3(x,y,t) = N_{u3}(x,y)\{q(t)\}, \tag{17}$$

$$v_1(x,y,t) = N_{v1}(x,y)\{q(t)\} \tag{18}$$

and

$$v_3(x,y,t) = N_{v3}(x,y)\{q(t)\}, \tag{19}$$

where $q(t) = [u_{1i}, v_{1i}, u_{3i}, v_{3i}, w_i, w_{,xi}, w_{,yi}]^{\mathrm{T}}$ for $i = 1, 2, 3, 4$. $N_w(x, y)$, $N_{u1}(x, y)$, $N_{u3}(x, y)$, $N_{v1}(x, y)$, and $N_{v3}(x, y)$ are the shape functions of the plate element.

The strain energy and kinetic energy derived in the above section can be rewritten in terms of nodal displacement variables as follows:

$$V = \tfrac{1}{2}\{q(t)\}^{\mathrm{T}}([K_1] + [K_2] + [K_3] + [K_4] + [K_5])\{q(t)\}, \tag{20}$$

where

$$[K_1] = h_1 \int\int_A [N_1]^{\mathrm{T}}[D_{1p}][N_1]\,\mathrm{d}x\,\mathrm{d}y, \tag{21}$$

$$[K_2] = \int\int_A [N_b]^{\mathrm{T}}[D_{1b}][N_b]\,\mathrm{d}x\,\mathrm{d}y, \tag{22}$$

$$[K_3] = h_3 \int\int_A [N_3]^{\mathrm{T}}[D_{3p}][N_3]\,\mathrm{d}x\,\mathrm{d}y, \tag{23}$$

$$[K_4] = \int\int_A [N_b]^{\mathrm{T}}[D_{3b}][N_b]\,\mathrm{d}x\,\mathrm{d}y \tag{24}$$

and

$$[K_5] = G_2 h_2 \times \int\int_A [N_g]^{\mathrm{T}}[N_g]\,\mathrm{d}x\,\mathrm{d}y, \tag{25}$$

where

$$[N_1] = \begin{bmatrix} N_{u1,x} \\ N_{v1,y} \\ N_{u1,y} + N_{v1,x} \end{bmatrix},$$

$$[N_b] = \begin{bmatrix} N_{w,xx} \\ N_{w,yy} \\ 2N_{w,xy} \end{bmatrix},$$

$$[N_3] = \begin{bmatrix} N_{u3,x} \\ N_{v3,y} \\ N_{u3,y} + N_{v3,x} \end{bmatrix},$$

$$[N_g] = \frac{d}{h_2}\begin{bmatrix} (N_{u1} - N_{u3})/d + N_{w,x} \\ (N_{v1} - N_{v3})/d + N_{w,y} \end{bmatrix},$$

$$[D_{ip}] = \frac{E_i}{(1 - \upsilon_i^2)}\begin{bmatrix} 1 & \upsilon_i & 0 \\ \upsilon_i & 1 & 0 \\ 0 & 0 & (1 - \upsilon_i)/2 \end{bmatrix}, \quad i = 1, 3,$$

$$[D_{ib}] = \frac{E_i I_i}{(1-\upsilon_i^2)} \begin{bmatrix} 1 & \upsilon_i & 0 \\ \upsilon_i & 1 & 0 \\ 0 & 0 & (1-\upsilon_i)/2 \end{bmatrix}, \quad i = 1, 3,$$

where E_i, υ_i, and I_i denote Young's modulus, Poisson's ratio, and the area moment of inertia of the ith layer.

In addition, the kinetic energy of the sandwich plate is

$$T = \tfrac{1}{2}\{\dot{q}(t)\}^{\mathrm{T}}([M_1] + [M_2] + [M_3] + [M_4])\{\dot{q}(t)\}, \tag{26}$$

where

$$[M_1] = \int \int_A (\rho_1 h_1 + \rho_2 h_2 + \rho_3 h_3)[N_w]^{\mathrm{T}}[N_w]\,\mathrm{d}x\,\mathrm{d}y, \tag{27}$$

$$[M_2] = \int \int_A \rho_1 h_1([N_{u1}]^{\mathrm{T}}[N_{u1}] + [N_{v1}]^{\mathrm{T}}[N_{v1}])\,\mathrm{d}x\,\mathrm{d}y, \tag{28}$$

$$[M_3] = \int \int_A \rho_3 h_3([N_{u3}]^{\mathrm{T}}[N_{u3}] + [N_{v3}]^{\mathrm{T}}[N_{v3}])\,\mathrm{d}x\,\mathrm{d}y, \tag{29}$$

$$[M_4] = \int \int_A I_2[N_g]^{\mathrm{T}}[N_g]\,\mathrm{d}x\,\mathrm{d}y. \tag{30}$$

Considering the situation of a sandwich plate element with a periodic load. The work done by the periodic load can be expressed as

$$W = \frac{1}{2}\int \int_A P(t)\left(\frac{\partial w}{\partial x}\right)^2 \mathrm{d}x\,\mathrm{d}y. \tag{31}$$

Substitute the interpolation function into the above equation, and we can obtain that

$$W = \tfrac{1}{2}\{q(t)\}^{\mathrm{T}} P(t)[K_g^e]\{q(t)\}, \tag{32}$$

where

$$[K_g^e] = \int \int_A \left[\frac{\partial N_W}{\partial x}\right]^{\mathrm{T}} \left[\frac{\partial N_W}{\partial x}\right] \mathrm{d}x\,\mathrm{d}y.$$

According to the Hamilton's principle, we have

$$\delta \int_{t_1}^{t_2} (T - V + W)\,\mathrm{d}t = 0. \tag{33}$$

By substituting the strain energy, kinetic energy, and the work done by the load force into the Hamilton's principle, the governing equation for the sandwich plate element is obtained as follows:

$$[M^e]\{\ddot{q}(t)\} + ([K^e] - P(t)[K_g^e])\{q(t)\} = \{0\}, \tag{34}$$

where

$$[M^e] = [M_1] + [M_2] + [M_3] + [M_4] \tag{35}$$

and

$$[K^e] = [K_1] + [K_2] + [K_3] + [K_4] + [K_5]. \tag{36}$$

Assembling the contributions of all elements, the global dynamic equation of the sandwich plate with an ER layer and constraining layer as shown in Fig. 5 can be expressed as

$$[M]\{\ddot{q}(t)\} + ([K] - P(t)[K_g])\{q(t)\} = \{0\}. \tag{37}$$

In the above equation, the periodic load force $P(t)$ can be expressed in the form

$$P(t) = \alpha P_0 + \beta P_0 \cos \Theta t, \tag{38}$$

where α is the static load factor, β is the dynamic load factor, Θ is the disturbance frequency, and P_0 is the static buckling load.

Substituting Eq. (38) into Eq. (37), the equation of motion can be rewritten as

$$[M]\{\ddot{q}(t)\} + ([K] - \alpha P_0[K_g] - \beta P_0[K_g] \cos \Theta t)\{q(t)\} = \{0\}. \tag{39}$$

The above equation is a Mathieu–Hill equation with a periodic coefficient. The boundary of the dynamic instability of the system is formed by the periodic situations of the T and $2T$, where $T = (2\pi/\Theta)$. The boundary of the primary instability region with period $2T$ is of practical importance and the solution can be obtained in the form as follows:

$$\{q(t)\} = \{a\} \sin(\Theta t/2) + \{b\} \cos(\Theta t/2). \tag{40}$$

Then, substitute Eq. (40) into Eq. (39) and the following relations can be obtained:

$$\left(-\frac{\Theta^2}{4}[M] + [K] - \alpha P_0[K_g] + \frac{\beta P_0}{2}[K_g]\right)\{a\} \sin(\Theta t/2) = \{0\}, \tag{41}$$

$$\left(-\frac{\Theta^2}{4}[M] + [K] - \alpha P_0[K_g] - \frac{\beta P_0}{2}[K_g]\right)\{b\} \cos(\Theta t/2) = \{0\}, \tag{42}$$

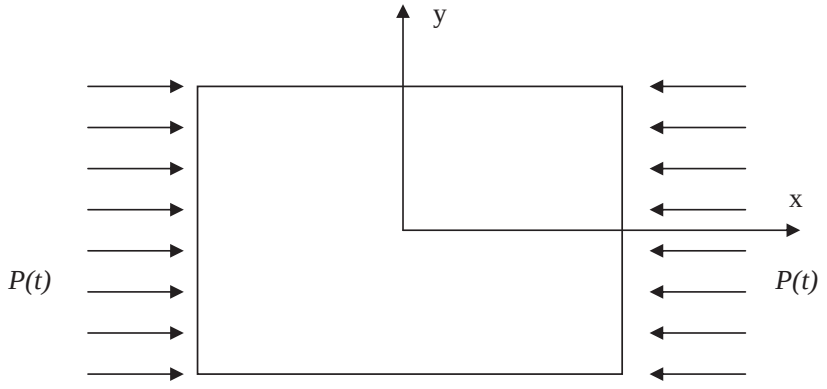

Fig. 5. A plate subjected to an in-plane dynamic load.

where the $\sin(\Theta t/2)$ and $\cos(\Theta t/2)$ can be expressed as exponential types:

$$\sin(\Theta t/2) = -\frac{\mathrm{j}}{2}[\exp(\mathrm{j}\Theta t) - \exp(-\mathrm{j}\Theta t)], \tag{43}$$

$$\cos(\Theta t/2) = \tfrac{1}{2}[\exp(\mathrm{j}\Theta t) + \exp(-\mathrm{j}\Theta t)], \tag{44}$$

where $\mathrm{j} = \sqrt{-1}$.

Substitute Eqs. (43) and (44) into Eqs. (41) and (42) and rewrite the above relations. The following equations can be obtain as:

$$\mathrm{j}\left(-\frac{\Theta^2}{4}[M] + [K^r] - \alpha P_0[K_g] + \frac{\beta P_0}{2}\right)\{a\} - [K^j]\{a\} = 0, \tag{45}$$

$$\mathrm{j}[K^j]\{b\} + \left(-\frac{\Theta^2}{4}[M] + [K^r] - \alpha P_0[K_g] - \frac{\beta P_0}{2}\right)\{b\} = 0, \tag{46}$$

where superscripts r and j of the stiffness matrices denote the real and imaginary part of matrices, respectively. The non-trivial solution of the system is as follows:

$$\begin{vmatrix} -\frac{\Theta^2}{4}[M] + [K^r] - P_0(\alpha - \beta/2)[K_g] & [K^j] \\ -[K^j] & -\frac{\Theta^2}{4}[M] + [K^r] - P_0(\alpha + \beta/2)[K_g] \end{vmatrix} = 0. \tag{47}$$

The above equation is referred to as the equation of boundary frequencies hereafter. It is used to calculate the boundaries of the instability regions of the system.

3. Numerical results and discussion

The dynamic stability problems of a sandwich plate with an ER fluid core and constrained layer are studied by finite element method. Existing models developed for viscoelastically damped sandwich structures were found applicable to ER material structural analysis due to the similarities in the rheological behavior. To validate the proposed algorithm and calculations, comparisons between the present results and the results of existing models are made first. The solutions of natural frequencies and loss factors of a simply supported sandwich plate with a viscoelastic layer are obtained. The numerical results are compared with those obtained by Lall et al. [20] and Zhang and Sainsbury [21] in Tables 1 and 2, respectively. The solutions solved by present model are shown to have a good accuracy. A good agreement can be observed in the above results with different geometry. And to validate the characteristics of the ER materials of the system, Fig. 6 shows the variations in the structural loss factor as a function of electric field and it can be seen that a good agreement with Choi et al. [12] at lower electric fields and Yalcintas and Dai [17] at higher electric fields.

Table 1
Comparisons of natural frequency and loss factor

	Ref. [18]		Present	
Mode	Natural frequency (rad/s)	Loss factor	Natural frequency (rad/s)	Loss factor
(1,1)	975.17	0.044	972.89	0.044
(1,2)	2350.79	0.019	2346.45	0.019
(2,1)	2350.79	0.019	2346.45	0.019
(2,2)	3725.33	0.012	3711.90	0.012

Table 2
Comparisons of natural frequency and loss factor

	Ref. [19]		Present	
Mode	Natural frequency (Hz)	Loss factor	Natural frequency (Hz)	Loss factor
1	59.05	0.206	58.69	0.201
2	113.67	0.213	113.75	0.211
3	128.89	0.207	129.16	0.208
4	175.76	0.188	175.46	0.189
5	193.67	0.179	193.79	0.183

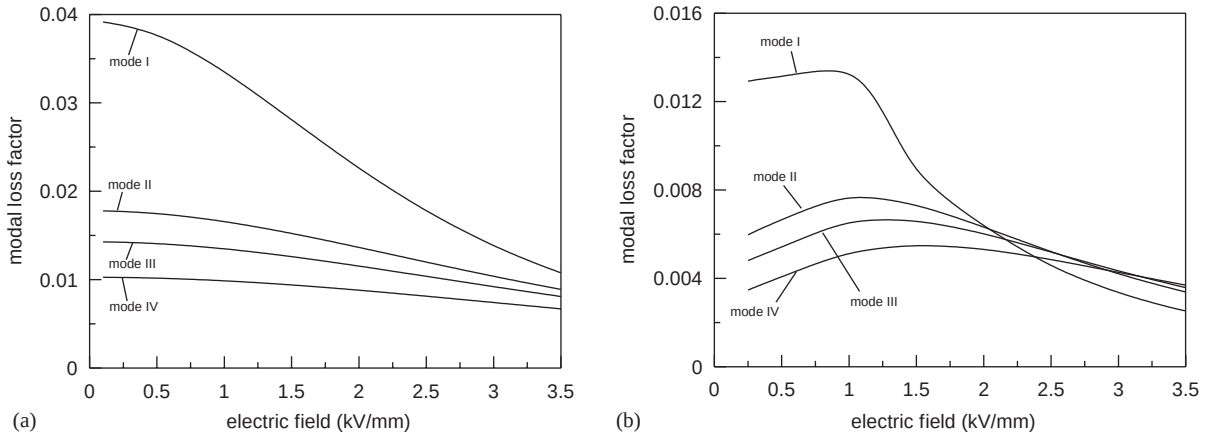

Fig. 6. Dependence of modal loss factor on the electric field for a sandwich plate with simply supported end condition ($h_1 = 0.05\,\text{mm}, h_2 = h_3 = 0.5\,\text{mm}$). (a) ER material by Don [22], (b) ER material by the modified experimental data [14].

The materials of the constrained layer and the plate are chosen to be aluminum. The geometrical and physical parameters of the sandwich plate are as follows:

$$a = 0.3\,\text{m}, \quad b = 0.25\,\text{m}, \quad E_1 = E_3 = 70 \times 10^9\,\text{N/m}^2, \quad \rho_1 = \rho_3 = 2700\,\text{kg/m}^3,$$

$$h_1 = 0.05\,\text{mm}, \quad h_2 = h_3 = 0.5\,\text{mm}, \quad \rho_2 = 1700\,\text{kg/m}^3, \quad \mu = 0.3.$$

The simply supported sandwich plate subjected to a in-plane dynamic load is chosen in Fig. 5. Besides, ω^* is the natural frequency of the simply supported sandwich plate with thickness ratio $h_1/h_3 = 0.1$, $h_2/h_3 = 0.5$, thickness of the base plate $h_3 = 0.5\,\text{mm}$ subjected to an electric field $E_* = 0.5\,\text{kV/mm}$. Based on the existing information of the ER material, only the electric field dependence properties of an ER material in the pre-yield regime needs to be considered. The complex modulus of the used ER fluid was experimentally measured by Don [22] and can be expressed as follows:

$$G_{2a} = G'_a + G''_a,$$

where the shear storage modulus $G'_a \approx 15\,000E_*^2$, the loss modulus $G''_a \approx 6900$, and E_* is the electric field in kV/mm.

Yalcintas [15] presented another modified experimental data to calculate the characteristics of the ER material and by the following relations:

$$G_{2b} = G'_b + G''_b,$$

where the shear storage modulus $G'_b \approx 50\,000E_*^2$, the loss modulus $G''_b \approx 2600E_* + 1700$.

Fig. 6 shows the variations in the structural loss factor for each mode as a function of electric field. We can see that the structural loss factor decreases as the elastic field increase as shown in Fig. 6(a). In Fig. 6(b), the modified ER material data is used to calculate the variations in the structural loss factor for each mode and It can be observed that the modal loss factor increases as the electric field increases and then decreases as the field becomes higher than a certain value about 1 kV/mm. The variations of the ER sandwich plate are similar with Choi et al. [12] in lower and higher electric fields, the variations of the structural loss factor of the sandwich plate are also similar. The electric field dependence of the loss factor is most significant in the first mode. The effects of the dynamic load factor β on the first dynamic instability regions are shown in Fig. 7.

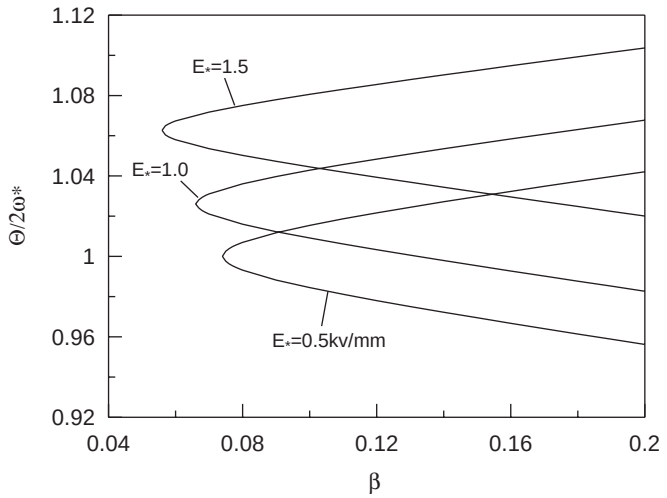

Fig. 7. The effects of dynamic load factor β with different applied electric fields ($h_1 = 0.05\,\text{mm}$, $h_3 = 0.5\,\text{mm}$, $h_2/h_3 = 0.5$).

The stability and instability boundaries are obtained by the first approximation in Eq. (47) and the primary instability regions are only drawn. The first instability regions of the sandwich plate will be moved upward by applying electric field as the stiffness of the ER layer is stronger at higher electric field, and the tip of first instability regions of the system decreases by decreasing the electric fields applied. Figs. 8 and 9 show the variations of the first instability regions with different thickness ratios (h_2/h_3) subjected to electric fields $E_* = 0.5$ and 1.5 kV/mm, respectively. As shown in the figures, it is found that the first instability regions of the system will be moved downward with the increasing of the thickness ratio (h_2/h_3). When the thickness of the ER layer

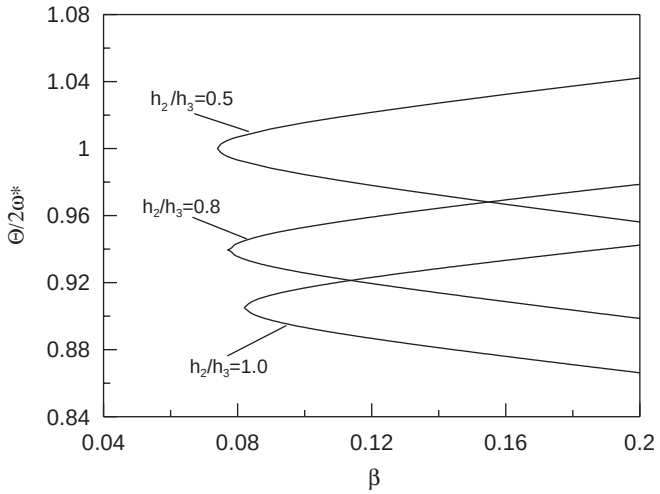

Fig. 8. The effects of dynamic load factor β with different thickness ratio h_2/h_3 ($h_1 = 0.05$ mm, $E_* = 0.5$ kV/mm).

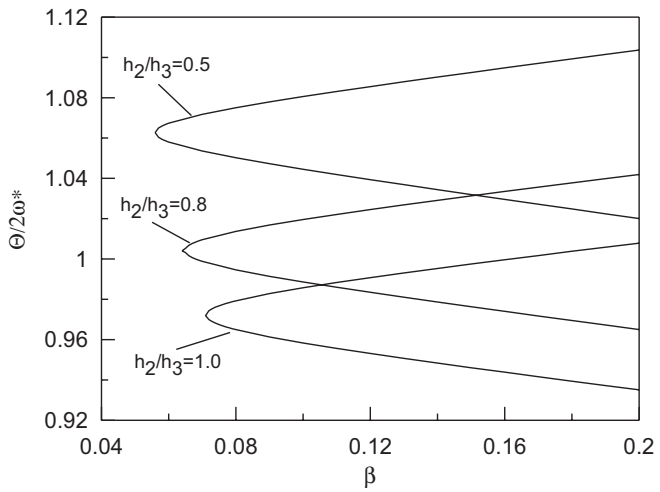

Fig. 9. The effects of dynamic load factor β with different thickness ratio h_2/h_3 ($h_1 = 0.05$ mm, $E_* = 1.5$ kV/mm).

increases, the first instability regions of the system will become smaller and are moved downward. The reasons are that the ER layer will provide a large damping effect as the thickness of the ER layer increases, and it will decrease the stiffness of the system too. So, the first instability regions of the system are moved downward and the damper of the system will be stronger. Additionally, it has the same results when applying different electric fields on the sandwich plate. And, the variations of the instability regions of the sandwich plate are more clear with changing the thickness of the ER fluid layer than changing the applied electric field. On the other hand, the effects of the constraining layer are also discussed in this study, and the variations of the first

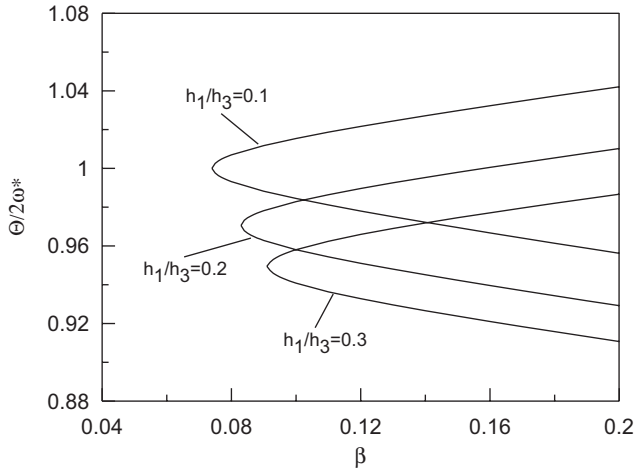

Fig. 10. The effects of dynamic load factor β with different thickness ratio h_1/h_3 ($h_2 = 0.05\,\text{mm}$, $E_* = 0.5\,\text{kV/mm}$).

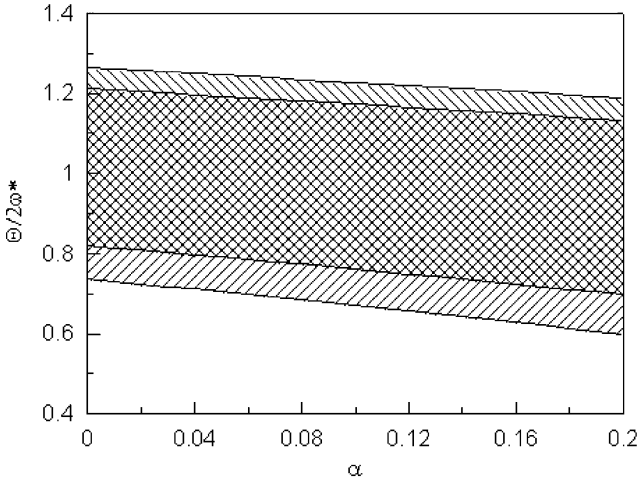

Fig. 11. The effects of static load factor α with different applied electric fields ($h_1 = 0.05\,\text{mm}$, $h_2 = h_3 = 0.5\,\text{mm}$, $E_* = 0.5\,\text{kV/mm}$: ▨; $E_* = 1.5\,\text{kV/mm}$: ▨) .

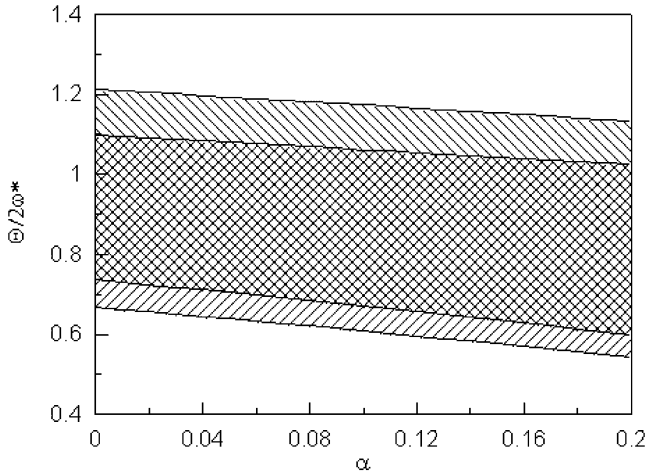

Fig. 12. The effects of static load factor α with different thickness ratio h_2/h_3 ($h_1 = 0.05\,\text{mm}$, $h_3 = 0.5\,\text{mm}$, $E_* = 0.5\,\text{kV/mm}$, $h_2/h_3 = 0.5$: ▨; $h_2/h_3 = 1.0$: ▧) .

instability regions of the system with different thickness of the constraining layer are plotted in Fig. 10. The constraining layer can also provide the damping effects as shown in the figure. The first instability region of the system will be moved downward and become smaller when the thickness of the constraining layer is getting larger. The effects of the static load factor α on the dynamic instability regions are shown in Fig. 11. In the figure, the first instability regions of the system are moved upward with increasing of applied electric fields. Fig. 12 shows the variations of the first instability regions when changing the thickness of the ER layer. From the results in Fig. 12, the stiffness of the system decreases with increasing of the thickness of the ER layer. The first instability regions will be moved downward as the stiffness of the system getting smaller when the thickness of the ER layer increases.

4. Conclusion

The dynamic stability problems of a sandwich plate with an ER fluid core and constrained layer are studied in this paper. The finite element method, and Bolotin's method are used in the analysis. Additionally, the complex representations of the ER fluid material are also used in this study. Numerical results are shown that the effects of the ER fluid layer and the constraining layer tend to stabilize plate system. It shows that the electric field will change the stiffness of the sandwich plate. The increase of the thickness of the ER layer will decrease the dynamic stability regions of the sandwich plate. The increase of the electric field level and the constraining layer thickness increases the stiffness of the sandwich plate, and it will change the instability regions of the system. Hence, the ER material can be used to improve the stability of various mechanical devices. The effects of the sandwich shell and circular plate with the ER fluid layer are the interesting topics to be studied. Additionally, the cases of the rotatory sandwich plates with ER fluid core are also an interesting one to be investigated.

References

[1] V.V. Bolotin, *The Dynamic Stability of Elastic System*, Holden-Day, San Francisco, 1964.
[2] R.M. Evan-Iwanowski, *Resonance Oscillations in Mechanical Systems*, Elsevier, Amsterdam, 1976.
[3] L. Briseghella, C. Pellegrino, Dynamic stability of elastic structures: a finite element approach, *Computers & Structures* 69 (1998) 11–25.
[4] K. Takahasi, Y. Konishi, Dynamic stability of rectangular plate subjected to distributed in-plane dynamic force, *Journal of Sound and Vibration* 123 (1) (1988) 115–127.
[5] P.J. Deolasi, P.K. Datta, Parametric instability characteristics of rectangular plates subjected to localized edge compressing (compression or tension), *Computers & Structures* 54 (1995) 73–82.
[6] R.S. Srinivasan, P. Chellapandi, Dynamic stability of rectangular laminated composite plates, *Computers & Structures* 24 (1986) 233–238.
[7] J. Moorthy, J.N. Reddy, Parametric instability of laminated composite plates with transverse shear deformation, *International Journal of Solids and Structures* 26 (1990) 801–811.
[8] L.W. Chen, J.Y. Yang, Dynamic stability of laminated composite plates by finite element method, *Computers & Structures* 36 (1990) 845–851.
[9] K.D. Weiss, J.P. Coulter, J.D. Carlson, Material aspects of electrorheological system, *Journal of Intelligent Material Systems and Structures* 4 (1) (1993) 13–34.
[10] D.A. Brooks, J. Goodwin, C. Hjelm, L. Marshall, C. Zukoski, Viscoelastic studies on an electro-rheological fluid, *Colloids and Surfaces* 18 (1986) 293–312.
[11] S.B. Choi, Y.K. Park, Active vibration control of cantilevered beam containing an electro-rheological fluid, *Journal of Sound and Vibration* 172 (1994) 428–432.
[12] S.B. Choi, Y.K. Park, S.B. Jung, Modal characteristics of a flexible smart plate filled with electrorheological fluids, *Journal of Aircraft* 36 (1999) 459–464.
[13] S.O. Oyadiji, Applications of electro-rheological fluids for constrained layer damping treatment of structures, *Journal of Intelligent Material Systems and Structures* 7 (1996) 541–549.
[14] J.P. Coulter, Engineering application of electrorheological material, *Journal of Intelligent Material Systems and Structures* 4 (1993) 248–259.
[15] M. Yalcintas, J.P. Coulter, Electrorheological material based adaptive beams subjected to various boundary conditions, *Journal of Intelligent Material Systems and Structures* 6 (1995) 700–717.
[16] M. Yalcintas, J.P. Coulter, Analytical modeling of electrorheological material based adaptive beams, *Journal of Intelligent Material Systems and Structures* 6 (1995) 488–497.
[17] M. Yalcintas, H. Dai, Magnetorheological and electrorheological materials in adoptive structures and their performance comparison, *Smart Materials & Structures* 8 (1999) 560–573.
[18] C.Y. Lee, Finite element formulation of a sandwich beam with embedded electro-rheological fluids, *Journal of Intelligent Material Systems and Structures* 6 (1995) 718–728.
[19] Y.K. Kang, J. Kim, S.B. Choi, Passive and active damping characteristics of smart electro-rheological composite beams, *Smart Materials & Structures* 10 (2001) 724–729.
[20] A.K. Lall, N.T. Asnani, B.C. Nakra, Vibration and damping analysis of rectangular plate with partially covered constrained viscoelastic layer, *Journal of Vibration, Acoustics, Stress, and Reliability in Design* 109 (1987) 241–247.
[21] Q.J. Zhang, M.G. Sainsbury, The Galerkin element method applied to the vibration of rectangular damped sandwich plate, *Computers & Structures* 74 (2000) 717–730.
[22] D.L. Don, An Investigation of Electrorheological Material Adoptive Structures, Master's Thesis, Lehigh University, Bethlehem, PA, 1993.